

Rugulactone and its Analogues Exert Antibacterial Effects through Multiple Mechanisms Including Inhibition of Thiamine Biosynthesis

Matthew B. Nodwell,^[a] Helge Menz,^[b, c] Stefan F. Kirsch,^[b, d] and Stephan A. Sieber^{*[a]}

Rugulactone is a dihydro- α -pyrone isolated from the plant *Cryptocarya rugulosa* in 2009. It has been reported to display I κ B kinase (IKK) inhibitory activity, as well as antibiotic activity in several strains of pathogenic bacteria. However, its biological targets and mode of action in bacteria have not yet been explored. Here we present enantioselective syntheses of rugulactone and of some corresponding activity-based protein profiling (ABPP) probes. We found that the ABPP probes in this study are more potent than rugulactone against *Staphylococcus aureus* NCTC 8325, *S. aureus* Mu50, *Listeria welshimeri* SLCC 5334 and *Listeria monocytogenes* EGD-e, and that molecules of this class probably exert their antibacterial effect through a combination of targets. These targets include covalent inhibition of 4-amino-5-hydroxymethyl-2-methylpyrimidine phosphate (HMPP) kinase (ThiD), which is an essential component of the thiamine biosynthesis pathway in bacteria. This represents the first example of a small-molecule inhibitor of ThiD.

cus aureus NCTC 8325, *S. aureus* Mu50, *Listeria welshimeri* SLCC 5334 and *Listeria monocytogenes* EGD-e, and that molecules of this class probably exert their antibacterial effect through a combination of targets. These targets include covalent inhibition of 4-amino-5-hydroxymethyl-2-methylpyrimidine phosphate (HMPP) kinase (ThiD), which is an essential component of the thiamine biosynthesis pathway in bacteria. This represents the first example of a small-molecule inhibitor of ThiD.

Introduction

Natural products possess unique molecular properties that distinguish them from libraries of synthetic compounds, and by virtue of their coevolution with biological systems, the structures can be considered “pre-validated”. Heroic efforts have been made in the field of the isolation and synthesis of natural products, but in many cases their application as drugs is hindered because the precise mechanisms of action and suites of targets are unknown. Rugulactone (Scheme 1) was isolated in 2009 from the plant *Cryptocarya rugulosa*^[1] and reported to exhibit antibacterial activities.^[2] The scaffold includes two potential Michael acceptors: an α,β -unsaturated γ -lactone, which is a system known to modify proteins, as in the cases of leptomycin B and ratjadone,^[3] together with an α,β -unsaturated ketone. The presence of two electrophilic groups suggests that rugulactone exerts its biological effects through inhibition of its target proteins based on a covalent mechanism. There are several published syntheses of rugulactone, but its biological targets or mechanism of action in bacteria have not to date been explored. In this account we report new asymmetric syntheses of rugulactone and of related probes and subsequently the application of these tool compounds to unravelling of their corresponding cellular targets by activity-based protein profiling.^[4]

Several syntheses of rugulactone have already appeared in the scientific literature. The key step—the introduction of the single chiral centre at C-6—has been achieved variously by use of a chiral pool approach,^[5] proline-catalysed α -aminoxylation of alcohols,^[2] Jacobsen’s hydrolytic kinetic resolution of epoxides,^[6] Keck asymmetric allylation^[7] or allylation of carbonyl compounds with chiral boronic esters.^[8] In our syntheses of rugulactone and of probes, we utilized asymmetric catalytic Overman esterification^[9] as the crucial step (Scheme S1 in the Supporting Information). The use of this reaction as the key

step is advantageous because of the commercial availability of the catalyst, as well as the ease of experimental setup.

One key consideration was the introduction of an alkyne handle for subsequent target analysis. In the interests of keeping the ABPP probes as structurally similar to rugulactone as possible, we attached the alkyne directly to the C-16 position of the appended aryl ring—distant from the Michael acceptors in the molecule. A retrosynthetic analysis of rugulactone and ABPP analogues is shown in Scheme 2A.

Results and Discussion

Our synthesis commenced with trichloroacetimidate **1**^[10] (Scheme 2B). Attempts to form the desired product **4** through asymmetric Overman esterification of **1** with vinylacetic acid failed. Treatment of **1** with benzoic acid (3 equiv) in the presence of (S)-(+)-COP-OAc (1.5 mol%) thus provided ester **2** in excellent yield and enantioselectivity as determined by chiral

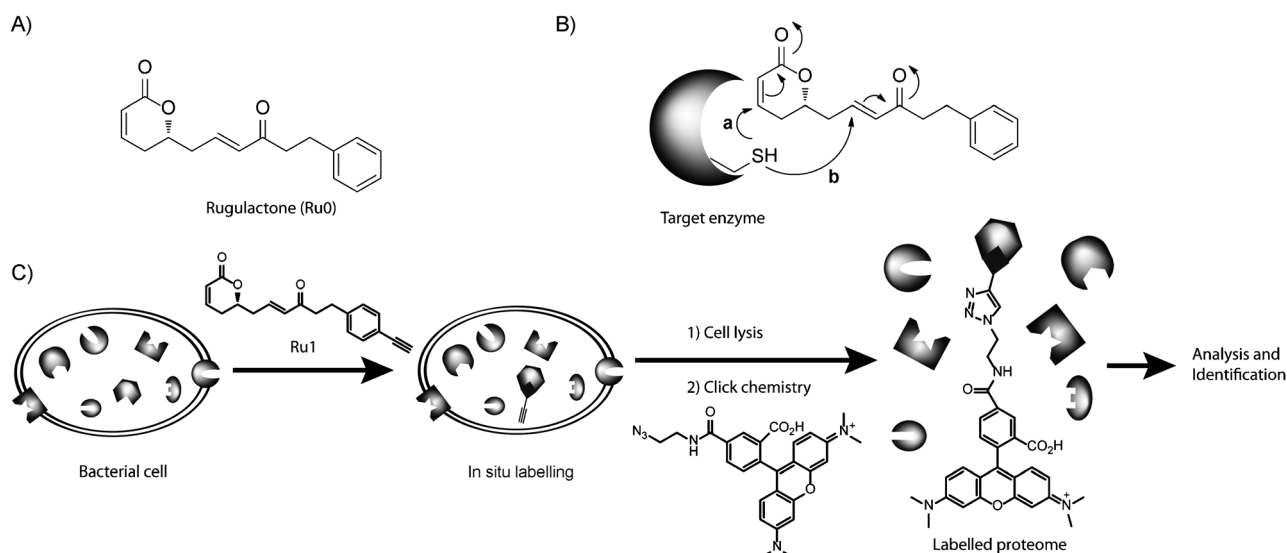
[a] M. B. Nodwell, S. A. Sieber
Department Chemie, Centre for Integrated Protein Science CIPSM
Institute of Advanced Studies, Technische Universität München
Lichtenbergstrasse 4, 85747, Garching (Germany)
E-mail: stephan.sieber@tum.de

[b] H. Menz, S. F. Kirsch
Department Chemie und Catalysis Research Center Munich
Lichtenbergstrasse 4, 85747, Garching (Germany)

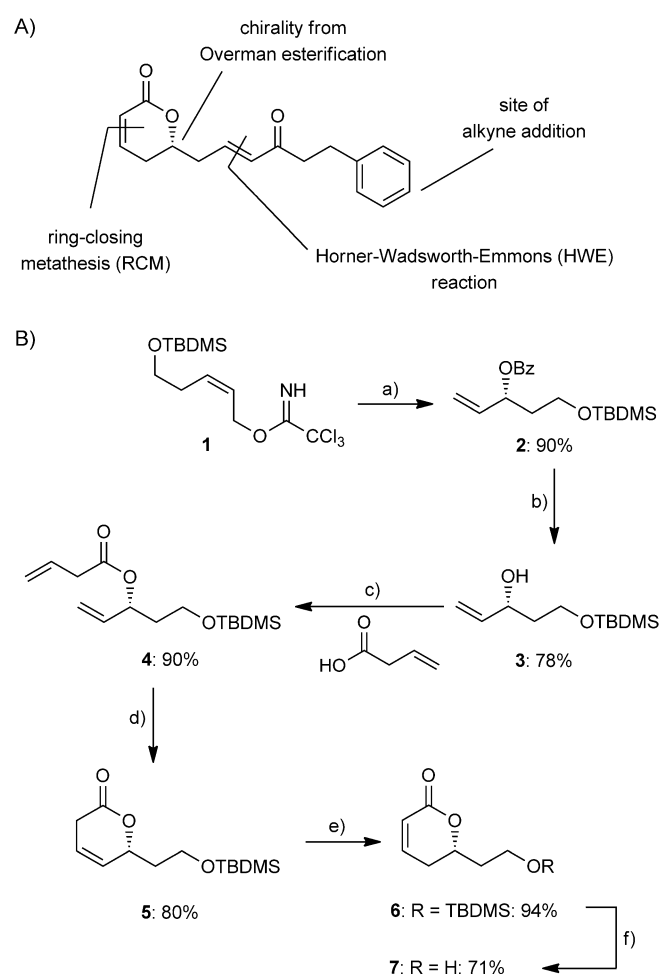
[c] H. Menz
Current address: BASF SE
Carl-Bosch-Strasse 38, GMT/S-B001 67056, Ludwigshafen (Germany)

[d] S. F. Kirsch
Current address: Bergische Universität Wuppertal, Organic Chemistry
Gaussstrasse 20, 42119, Wuppertal (Germany)

Supporting information for this article is available on the WWW under <http://dx.doi.org/10.1002/cbic.201200265>.



Scheme 1. A) Rugulactone (Ru0) structure. B) Thiol groups in the target enzyme's binding site can participate in Michael reactions either with the α,β -unsaturated γ -lactone in rugulactone (pathway a) or with the α,β -unsaturated ketone (pathway b). C) An alkyne function in an appropriately designed rugulactone probe allows the attachment of a tag to labelled enzymes. The conjugation of a rhodamine tag by click chemistry after cell lysis, allowing for fluorescent proteome visualization, is shown.



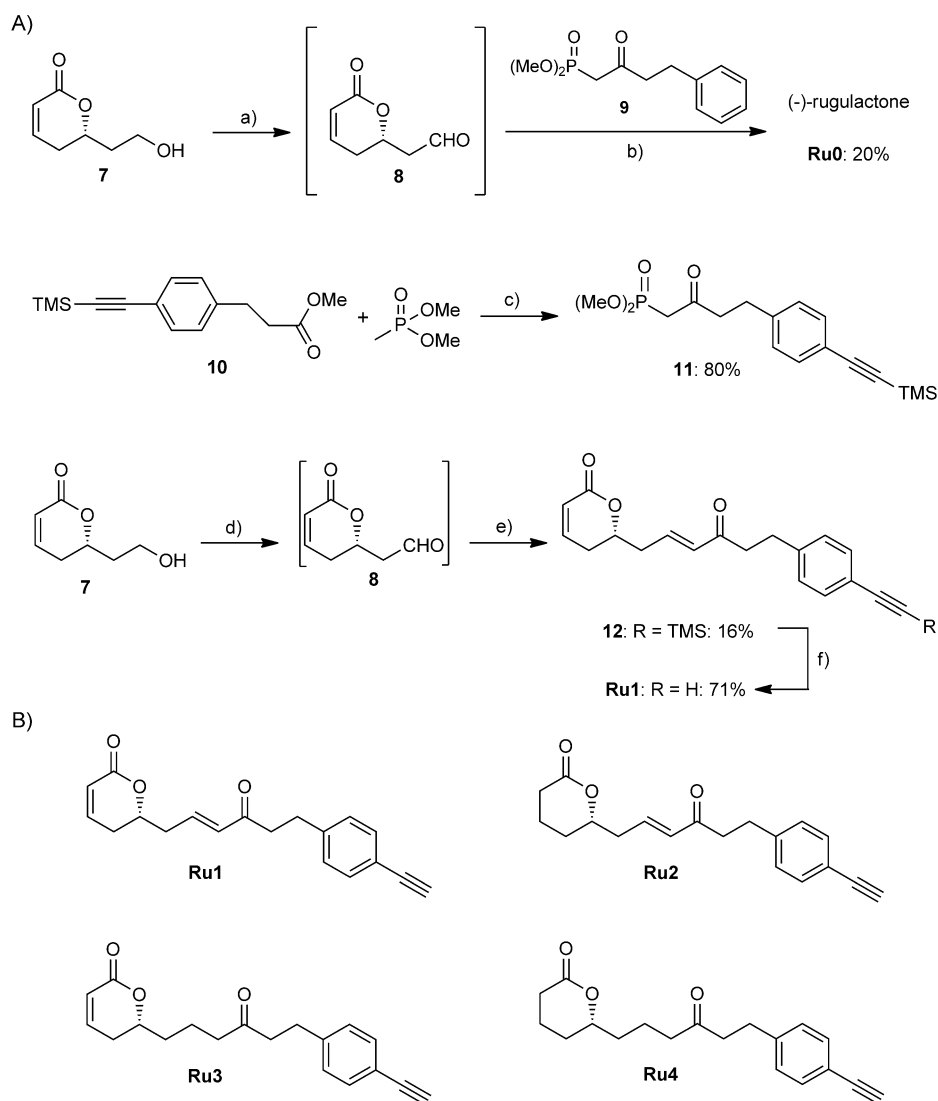
Scheme 2. A) Retrosynthetic analysis of rugulactone. B) Synthesis of primary alcohol 7. a) (S)-(+)-COP-OAc, BzOH, CH_2Cl_2 ; b) K_2CO_3 , MeOH; c) DIPC, DMAP, CH_2Cl_2 ; d) Grubbs II, Δ , CH_2Cl_2 ; e) DBU, CH_2Cl_2 ; f) HF/ CH_3CN .

HPLC (see the Supporting Information). Cleavage of the ester followed by coupling of the resultant alcohol, **3**, with vinylacetic acid yielded **4** in three steps. Standard ring-closing metathesis of **4** with the second-generation Grubbs catalyst yielded lactone **5**, which was isomerised to the desired α,β -unsaturated lactone **6** and deprotected to yield primary alcohol **7**. To complete the synthesis, treatment of phosphonate **9** with aldehyde **8** (generated in situ) gave (–)-rugulactone (Ru0) in moderate yield (Scheme 3 A).

For the synthesis of the alkyne-containing rugulactone probes, phosphonate **11** was assembled by means of a reaction^[11] between dimethyl methylphosphonate and ester **10**. With **11** to hand, the oxidation of **7** and a subsequent Horner-Wadsworth-Emmons (HWE) reaction, followed by deprotection of the alkyne group in **12**, yielded probe Ru1.

We also synthesized reduced analogues Ru2, Ru3, and Ru4 in order to explore the contributions of the two Michael acceptors to the labelling and biological activity of rugulactone. The synthesis of these probes is shown in Schemes S2–S4. The structures of all the rugulactone probes used in this study are shown in Scheme 3 B.

With rugulactone (Ru0) and probes Ru1–4 to hand, we assessed their biological properties in *Staphylococcus aureus* NCTC 8325, multidrug-resistant *S. aureus* Mu50,^[12] *Listeria monocytogenes* EGD-e, *Listeria welshimeri* SLCC 5334, *Pseudomonas aeruginosa* PAO1 and *Pseudomonas putida* KT2440. An examination of the MIC values for Ru0–Ru4 (Table 1) reveals that addition of an alkyne tag (Ru0 to Ru1) results in a twofold increase in potency for the *Staphylococcus* and *Listeria* strains tested (800 μM for Ru0 vs. 400 μM for Ru1 in both strains). Reduction of the lactone Michael acceptor yields a molecule (Ru2) that is still more active than the natural product (600 μM), indicating that the ketone Michael acceptor is primarily responsible for antibacterial activity. Probes Ru3 and



Scheme 3. A) Synthesis of rugulactone (Ru0) and ABPP probe Ru1. B) Structures of the rugulactone ABPP probes used in this study. a) Pyr-SO_3 , DMSO, DIEA, CH_2Cl_2 , -20°C ; b) NaH, THF, -78°C ; c) LDA, THF, 0°C ; d) Pyr-SO_3 , DMSO, DIEA, CH_2Cl_2 , -20°C ; e) 11, NaH, THF, -78°C ; f) TBAF, THF, HOAc.

Ru4 were found to be inactive against all tested bacteria. Rugulactone and its ABPP probes were inactive against both *P. aeruginosa* and *P. putida*, which came as a surprise because rugulactone had previously been reported to show an MIC of $12.5\ \mu\text{g mL}^{-1}$ ($46\ \mu\text{M}$) against *P. aeruginosa*.^[2] The lack of antibacterial activity could be due either to a lack of appropriate targets in these organisms or to limited cell permeability.

In order to unravel the molecular mechanisms responsible for the antibacterial activity, we examined whole-cell labelling with our rugulactone probes. The probes were incubated with living bacteria and after one hour, excess probe was removed and the cells were lysed by sonication. A fluorescent azide-containing tag (RhN_3 , Figure S1) was then appended to the alkyne-labelled proteome through a Huisgen–Sharpless–Meldal cycloaddition (click chemistry),^[13] and the labelling was analysed by in-gel fluorescence scanning (Figure 1). An in vivo dose-down experiment determined that $200\ \mu\text{M}$ was a sufficient concentration for the full saturation of most of the observed protein targets (Figure S2). Additionally, thermal denaturation of the bacterial proteomes resulted in a loss of the visible protein bands, demonstrating that an active, folded protein is necessary for probe labelling (Figure S3). In order to unravel the identities of all target proteins, we applied a quantitative enrichment procedure by which living cells were incubated with Ru1, lysed and clicked to trifunctional rhodamine-biotin-azide linker (Rh-biotin-N_3 , Figure S1); this allows the selective enhancement of probe-labelled proteins through the use of avidin beads. Subsequent SDS-PAGE revealed protein bands, and these were isolated, digested with trypsin and subjected to mass spectrometry (LC-MS/MS analysis). The obtained peptide fragments were analysed with the aid of the SEQUEST search algorithm and identified enzymes are summarized in Figure 1 and Table S2.

A strong band observed only in *S. aureus* was identified as formate acetyltransferase (FAT), which contains eight cysteine

Table 1. MICs of Ru0–4 versus selected organisms in μM (mg mL^{-1}).

	<i>S. aureus</i> NCTC 8325	<i>S. aureus</i> Mu50	<i>L. monocytogenes</i> EGD-e	<i>L. welshimeri</i> SLCC 5334	<i>P. aeruginosa</i> PAO1	<i>P. putida</i> KT2440
Ru0	800 (0.22)	800 (0.22)	800 (0.22)	800 (0.22)	> 1000 (0.3)	> 1000 (0.3)
Ru1	400 (0.12)	400 (0.12)	400 (0.12)	400 (0.12)	> 1000 (0.3)	> 1000 (0.3)
Ru2	600 (0.18)	600 (0.18)	600 (0.18)	600 (0.12)	> 1000 (0.3)	> 1000 (0.3)
Ru3	> 1000 (0.3)	> 1000 (0.3)	> 1000 (0.3)	> 1000 (0.3)	> 1000 (0.3)	> 1000 (0.3)
Ru4	> 1000 (0.3)	> 1000 (0.3)	> 1000 (0.3)	> 1000 (0.3)	> 1000 (0.3)	> 1000 (0.3)

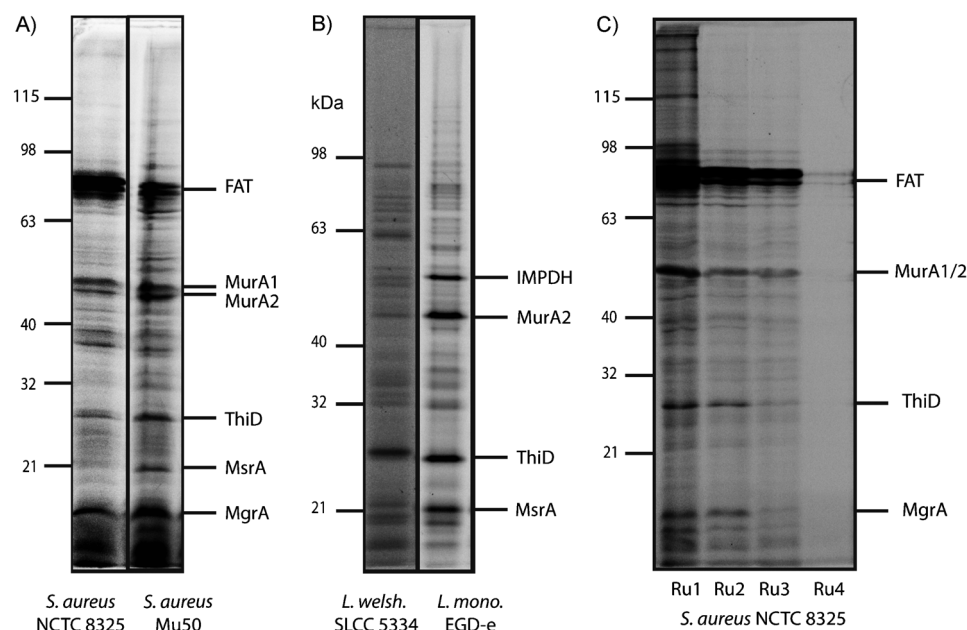


Figure 1. Labelling of bacterial proteomes with rugulactone probes as visualized by in-gel fluorescence scanning after click chemistry reaction with azide RhN_3 . Cytosolic fractions shown. Membrane fractions showed no bands. A) In vivo labelling of *S. aureus* NCTC 8325 and Mu50 with Ru1 (200 μM). B) In vivo labelling of *L. welshimeri* SLCC 5334 and *L. monocytogenes* EGD-e with Ru1 (200 μM). C) In vivo labelling of *S. aureus* NCTC 8325 with Ru1–Ru4 (200 μM). For abbreviations please refer to Table S2.

residues and is known to react strongly with Michael-acceptor-based probes.^[14] Furthermore, heat denaturation of this protein does not negate its reactivity towards Michael acceptors, indicating a predominantly unspecific labelling event. Further assessment of Figure 1 A and B reveals several interesting bacterial targets for probe labelling. MsrA (methionine sulfoxide reductase), for example, is absent from *S. aureus* NCTC 8325 and *L. welshimeri* SLCC 5334, yet is strongly labelled in these organisms' more virulent counterparts *S. aureus* Mu50 and *L. monocytogenes* EGD-e (Figure 1 A and B). Interestingly, MsrA has repeatedly been identified as a virulence factor in pathogenic organisms,^[15] whereas pathogens deficient in MsrA have been reported to have reduced ability to adhere with eukaryotic cells^[16] and to survive inside hosts.^[17] The key global regulator MgrA has been reported to control the expression of ≈ 350 genes in *S. aureus*^[18] and is labelled by Ru1 in both strains of *S. aureus* (Figure 1 A). As with MsrA, MgrA is also implicated in virulence regulation in pathogenic bacteria.^{[19][20]} The MsrA and MgrA hits were verified by recombinant expression, and subsequent labelling of these proteins with Ru1 indicated a specific binding event (Figure S4). In addition to these virulence regulators, several essential bacterial enzymes were also identified. MurA (UDP-*N*-acetylglucosamine-1-carboxyvinyl-transferase) catalyses the first committed step in cell wall biosynthesis. Low C+G Gram-positive bacteria possess two copies of MurA: MurA1 and MurA2.^[21] Gene deletion experiments demonstrate that removal of either gene results in a viable organism, but a double *murA1/murA2* knockout is lethal.^[21–22] We had previously demonstrated potent inhibition of MurA1 by the Michael-acceptor-containing compound

showdomycin; this probably contributes heavily to the antibacterial activity of this compound.^[14a] However, upon measurement of MurA1 inhibition with Ru0–Ru4, only very weak inhibition was observed: Ru1, for example, shows $\approx 50\%$ inhibition at 300 μM (Figure S5). To evaluate the effect on MurA2, we recombinantly expressed the enzyme (solubilised in the membrane fraction, Figure S6) and measured its inhibition with probes Ru0–4. The IC_{50} values and dose response curves are presented in Figure 2 and Table 2.

Neither Ru3 nor Ru4 displayed any activity versus MurA2 at any of the concentrations tested. Ru0–Ru2 inhibited MurA2 to much greater extents than MurA1, and the IC_{50} values from this assay correlate with MIC values, indicating that inhibition of MurA2, in concert with weak

MurA1 activity, is a possible contributor to the antibacterial activities of the rugulactone compounds.

Finally, we turned our attention to the strongly labelled band identified as ThiD. ThiD (HMPP kinase) is an essential dual-function enzyme in the thiamine biosynthesis pathway that catalyses the phosphorylation reactions of HMP and HMPP (Scheme 4) to form HMPPP, which is then used in a coupling reaction to form thiamine phosphate.^[23]

Thiamine (vitamin B1) is present in all living organisms as an essential cofactor of several key enzymes. Humans and other mammals depend solely on uptake of thiamine from their diet, whereas plants, bacteria and the protozoan parasite *Plasmodium* obtain thiamine by a combination of de novo biosynthesis and various salvage pathways.^[23] As shown in Figure 1 A and B, ThiD is labelled strongly by Ru1 in *L. monocytogenes* and *S. aureus*. Furthermore, an examination of Figure 1 C reveals that in susceptible bacteria (*S. aureus* NCTC 8325 shown), only the biologically active probes Ru1 and Ru2 label ThiD. These data indicate that the inhibition of ThiD might play a role in the antibacterial activity of rugulactone and its ABPP probes. To date, there are no reported small-molecule inhibitors of ThiD, but inhibition of thiamine biosynthesis is a potential source of antibacterial targets,^[24] particularly in organisms such as *Mycobacterium tuberculosis*, which lack salvage pathways as well as transporters of thiamine, eliminating the possibility of environmental uptake.^[25] The significance of ThiD in *L. monocytogenes* metabolism has been established: deletion mutants of *thiD* in this organism displayed a 3.3-fold reduction in epithelial intracellular growth—presumably a consequence of a thiamine-depleted environment.^[26] The inhibition of recombinant

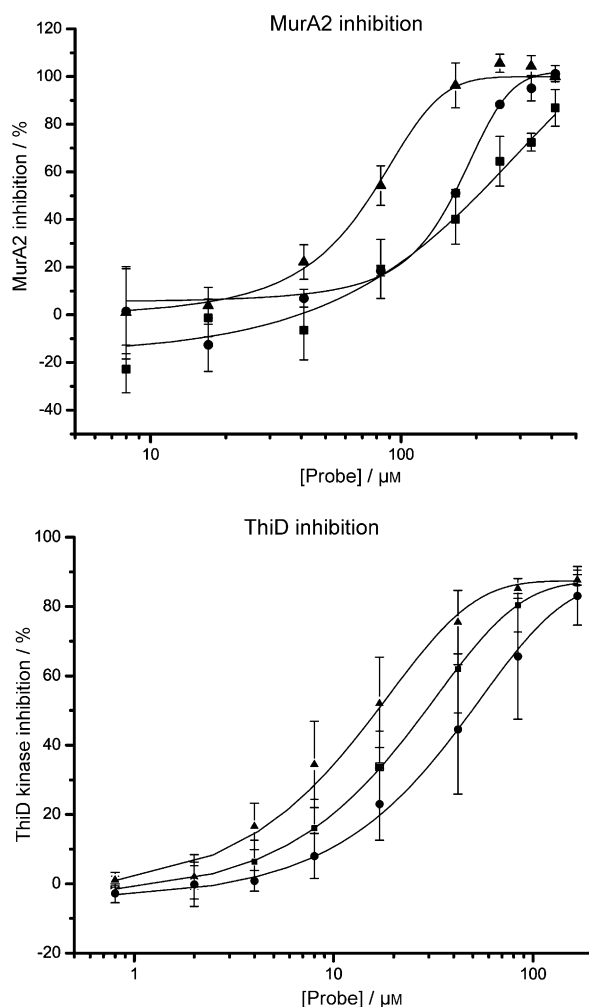


Figure 2. Dose–response curves for rugulactone probes against MurA2 and ThiD, together with IC_{50} values for each inhibitor. \blacktriangle : Ru1, \blacksquare : Ru0, \bullet : Ru2, N/A: not applicable.

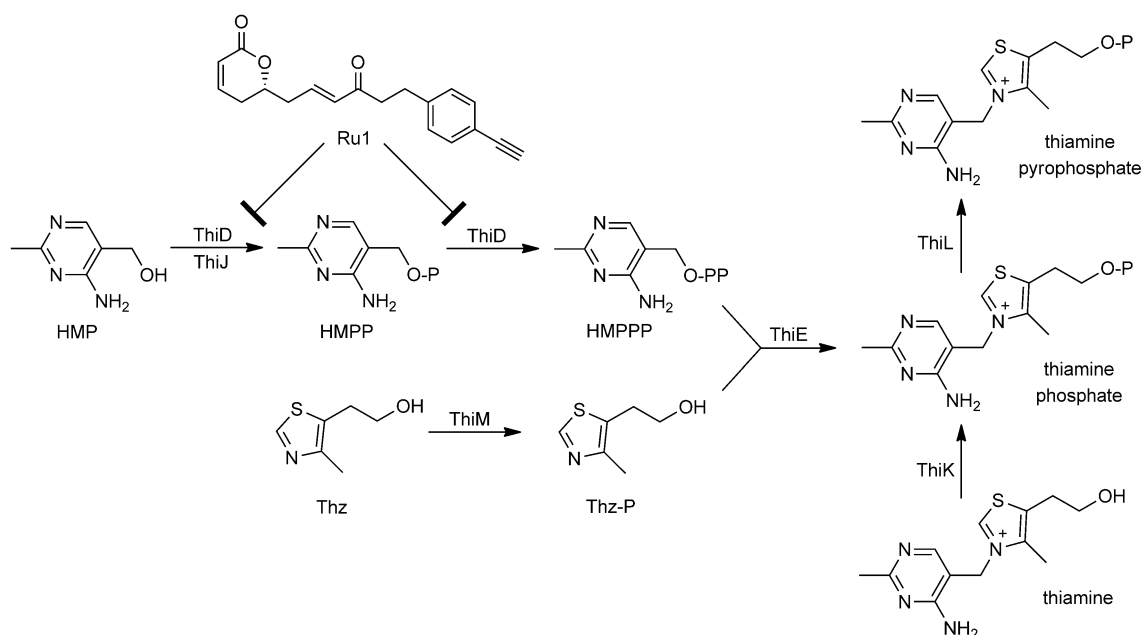
Table 2. IC_{50} values [μ M] for inhibitors Ru0–Ru4.

Compound	IC_{50} [μ M]	
	<i>S. aureus</i> Mu50 Mur A2	<i>S. aureus</i> Mu50 ThiD
Ru0	~400	25
Ru1	90	14
Ru2	150	32
Ru3	n.a.	n.a.
Ru4	n.a.	n.a.

n.a.: not applicable.

purified ThiD from *S. aureus* Mu50 by rugulactone and its ABPP probes was assayed with the aid of a pyruvate kinase/lactate dehydrogenase coupled enzyme system.^[27] The dose–response curves and IC_{50} values for this assay are shown in Figure 2 and Table 2.

Neither Ru3 nor Ru4 showed any HMPP kinase inhibition at any of the concentrations tested. Interestingly, though, potent inhibition, ranging from 14 to 32 μ M, was observed for Ru0–Ru2; this correlates well with the observed labelling pattern. These compounds therefore represent the first known small-molecule inhibitors of ThiD. In order to assess the contribution of ThiD inhibition by Ru1 to antibacterial activity, we compared MIC values of *L. monocytogenes* EGD-e in chemically defined media (CDM) with and without thiamine. *L. monocytogenes* is known to be capable of thiamine uptake, so a drop in MIC for Ru1 should be observed if no environmental thiamine can be salvaged. To our satisfaction, the MIC of Ru1 for *L. monocytogenes* EGD-e grown in CDM without thiamine was approximately four times lower than that of *L. monocytogenes* grown in thiamine-containing CDM (25 and 100 μ M, respectively), demonstrating the significance of ThiD inhibition for antibacterial activity (Figure S7). In biological systems, Michael acceptors



Scheme 4. Prokaryotic thiamine biosynthetic pathway. Inhibition of the essential enzyme ThiD by Ru1 would block de novo thiamine biosynthesis.

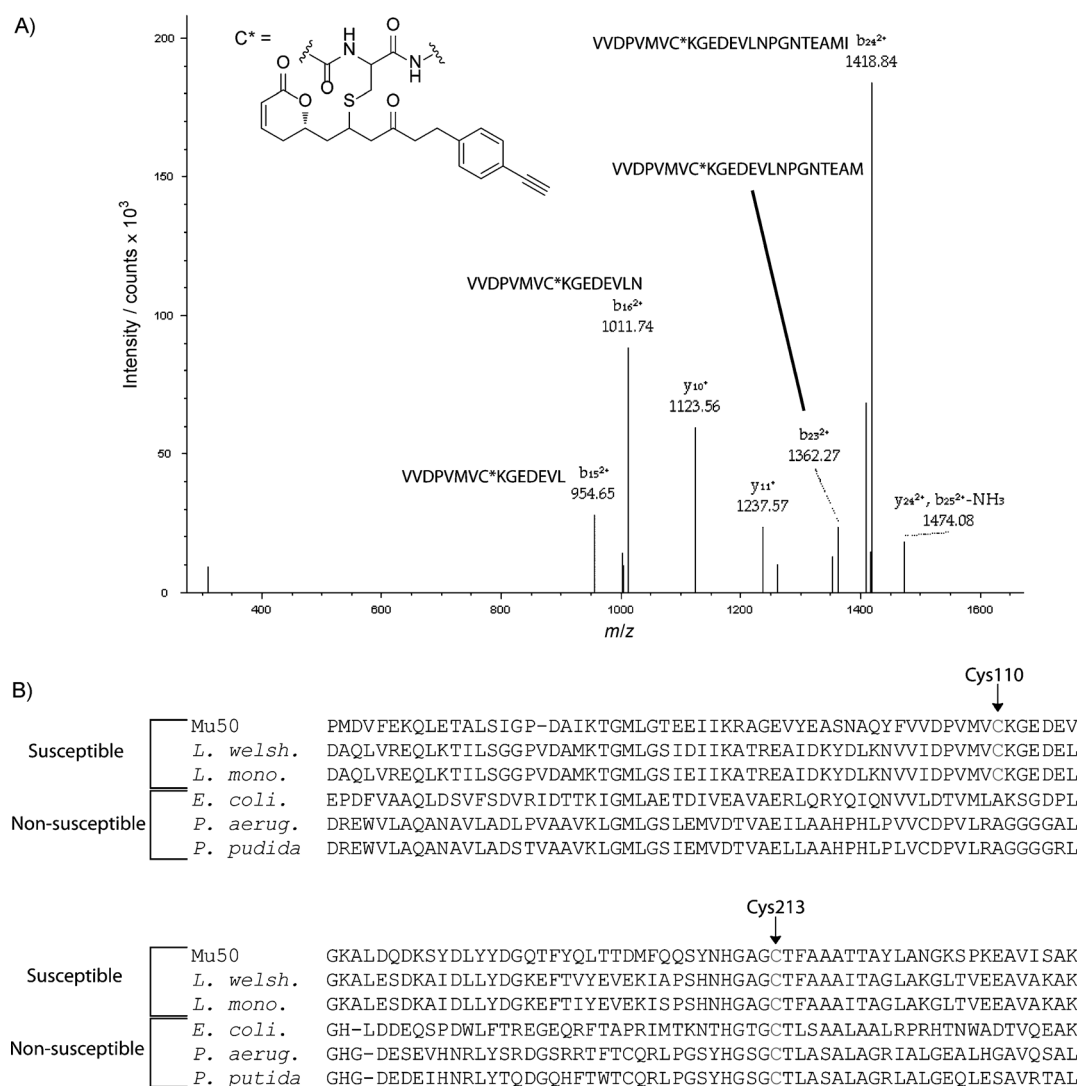


Figure 3. Identification of the binding site of Ru1 by mass spectrometry. A) MS fragmentation pattern for ThiD chymotryptic peptide VVDPVMVC*KGEDEVLPNGNTEAMI. B) Sequence alignment of ThiD from various organisms.

overwhelmingly react with the thiol moieties in cysteine residues.^[28] It is therefore very likely that rugulactone and its probes modify ThiD at a cysteine residue. A crystal structure of ThiD from *Salmonella typhimurium* reveals an active site cysteine (Cys213) that is highly conserved amongst HMPP kinases.^[29] However, labelling of recombinant ThiD with Ru1 followed by digestion and examination of the (chymo)tryptic peptides by LC-MS/MS reveals that Cys110 is the site of modification of ThiD (Figure 3A). These data suggest allosteric inhibition of ThiD by Ru1. Interestingly, BLAST comparisons of *S. aureus* (Mu50 and NCTC 8325), *L. monocytogenes* EGD-e, *P. aeruginosa* PAO-1, *P. putida* KT2440 and *Escherichia coli* K12 ThiD show that in the susceptible bacteria, Cys110 is conserved, whereas in *P. aeruginosa* and other non-susceptible organisms it is not (Figure 3B). Unfortunately, Cys110 is not conserved in *M. tuberculosis*, but further studies are needed to confirm a lack of ThiD inhibition in this organism.

Conclusions

In conclusion, we report syntheses of the natural product rugulactone and of its related ABPP probes. Probes Ru1 and Ru2 display substantially more antibacterial activity than the natural product, despite relatively small perturbations in structure. The observed bioactivity and labelling patterns of Ru1–Ru4 suggest that the chemical reactivity and inhibitory power of rugulactone is largely contributed by the α,β -unsaturated ketone Michael acceptor systems present in Ru1 and Ru2. We have described probes Ru0–Ru2 as MurA2 inhibitors, as well as the first known examples of small-molecule inhibitors of ThiD. Furthermore, we have demonstrated that the inhibition of this enzyme contributes to its antibacterial activity against *L. monocytogenes* in a chemically defined medium; this is consistent with the growth behaviour of Δ thiD *L. monocytogenes* in epithelial cells.^[26] Rugulactone therefore represents an important core scaffold that exerts its antibacterial activity through multiple target interactions. With regard to antibacterial therapy,

this mode of action is preferred because resistance development against several targets is more difficult to achieve.

Experimental Section

Bacterial strains: *Staphylococcus aureus* strains NCTC 8325 (Institute Pasteur, France), Mu50/ATCC 700699 (Institute Pasteur, France), were maintained in brain–heart broth (BHB) medium at 37 °C. *Listeria monocytogenes* strains EGD-e (Institute Pasteur, France) and the nonpathogenic strain *Listeria welshimeri* SLCC 5334 serovar 6b (DSMZ, Germany) were maintained in BHB medium, whereas *Pseudomonas aeruginosa* PAO1 (Institute Pasteur, France) and *Pseudomonas putida* KT2440 (ATCC, USA) were maintained in lysogeny broth (LB) medium. All strains were grown at 37 °C.

MIC measurements: Overnight cultures of bacteria were diluted in fresh BHB or LB medium to give $OD_{600} = 0.01$, and aliquots (99 μ L) were incubated in Nunclon round-bottomed 96-well plates with the corresponding DMSO stocks of rugulactone and rugulactone probes (1 μ L) in varying concentrations. The samples were incubated overnight at 37 °C and the optical densities were obtained by visual inspection for MIC calculation. All experiments were conducted at least in triplicate, and DMSO served as control.

In vivo experiments

Analytical labelling: *S. aureus* NCTC 8325, *S. aureus* Mu50, *L. monocytogenes* EGD-e and *L. welshimeri* SLCC 5334 were grown in BHB (5 mL). All bacteria were harvested by centrifugation 1 h after reaching stationary phase. After washing with 1 \times PBS (pH 7.5), the cells were resuspended in PBS (100 μ L). The bacteria were then incubated at room temperature for 60 min with varying concentrations of probe in DMSO, with the final DMSO concentration not exceeding 2%. Subsequently, the cells were washed twice with PBS to remove excess probe, resuspended in PBS (100 μ L) and lysed by sonication with a Bandelin Sonopuls instrument (10 \times 30 s, 80% power) and ice cooling. The proteomes were then separated into cytosolic and membrane fractions by centrifugation (16 200 \times g, 30 min, 4 °C). The membrane fraction was washed with PBS (2 \times 500 μ L), with collection by centrifugation (16 200 \times g, 30 min, 4 °C) after each wash, then resuspended in PBS (100 mL). Click chemistry was then carried out on both fractions with rhodamine azide RhN₃, RhN₃ (10 mM, 2 μ L), tris(2-carboxyethyl)phosphine (TCEP, 60 mM, 2 μ L) and tris[(1-benzyl-1H-1,2,3-triazol-4-yl)methyl]amine (TBTA, 1.6 mM, 6 μ L) were added in succession to the lysate solution. The samples were gently vortexed, and the cycloaddition was initiated by the addition of CuSO₄ (50 mM, 2 μ L). The cycloaddition reaction was allowed to proceed for 1 h at room temperature, followed by the addition of 100 μ L 2 \times BME buffer [TRIS-HCl (496 mg), glycerine (5 mL), Bromophenol blue (1.25 mg), SDS (1 g), β -mercaptoethanol (2.5 mL) in H₂O (50 mL), pH 8.3]. This final solution (50 μ L) was applied to an SDS-PAGE gel, and the developed gel was visualized by in-gel fluorescence scanning with use of a Fujifilm Las-4000 luminescent image analyzer, a Fujinon VRF43LMD3 lens and a 575DF20 filter. Coomassie staining was then performed on the gels to gauge levels of protein expression.

Preparative labelling: Bacteria were grown in the same medium (10 mL) as described for analytical labelling. Cells were harvested 1 h after reaching stationary phase, washed and resuspended in PBS (200 μ L). Labelling was carried out with 200 μ M probe for 1 h at room temperature. The DMSO concentration did not exceed 2% in all experiments. After washing to remove excess probe, the cells were resuspended in PBS (200 μ L) and lysed by sonication as described above. The cytosolic and membrane fractions were separat-

ed, and click chemistry was carried out on the cytosolic fraction as described above with the rhodamine-biotin-azide Rh-biotin-N₃ [amounts used: Rh-biotin-N₃ (10 mM, 4 μ L), TCEP (60 mM, 4 μ L), TBTA (1.6 mM, 12 μ L), CuSO₄ (50 mM, 4 μ L)]. Reactions for enrichment were carried out together with a control lacking the probe to compare the results for the biotin-avidin-enriched samples with the background of unspecific protein binding on avidin-agarose beads. After click chemistry, proteins were precipitated by use of an equal volume of precooled acetone. Samples were stored on ice for 60 min and centrifuged at 16 200 \times g for 30 min at 4 °C. The supernatant was discarded, and the pellet was washed two times with cold methanol (0 °C, 500 μ L), with resuspension by sonication each time (2 \times 10 s, 40% power) and collection of the pellet each time by centrifugation (16 200 \times g, 30 min, 4 °C). Subsequently, the pellet was dissolved in SDS in PBS (0.2%, 1 mL) by sonication (3 \times 10 s, 40% power) and incubated with gentle mixing with avidin-agarose beads (Sigma–Aldrich, 50 μ L) for 1 h at room temperature. The beads were washed three times with SDS in PBS (0.2%, 1 mL), twice with urea (6 M, 1 mL), and three times with PBS (1 mL). Beads were collected after each wash by centrifugation at 2500 rpm for 1 min. Aliquots of 2 \times BME buffer (50 μ L) were added and the proteins were released for preparative SDS-PAGE by 6 min incubation at 95 °C. The whole aliquot was then applied to a preparative SDS-PAGE gel. Gel bands were isolated, washed and tryptically digested as described previously.^[30]

Acknowledgements

We thank Mona Wolf for excellent scientific support and Max Pitcheider for the *E. coli* clones. We also thank Tadhg Begley for the kind gift of HMP. S.A.S. was supported by the Deutsche Forschungsgemeinschaft, SFB749, FOR1406, an ERC starting grant and the Center for Integrated Protein Science, Munich (CIPSM). M.B.N. thanks the Alexander von Humboldt foundation for financial support.

Keywords: antibiotics • chemical biology • natural products • proteomics • rugulactone

- [1] T. L. Meragelman, D. A. Scudiero, R. E. Davis, L. M. Staudt, T. G. McCloud, J. H. Cardellina II, R. H. Shoemaker, *J. Nat. Prod.* **2009**, 72, 336–339.
- [2] D. K. Reddy, V. Shekhar, P. Prabhakar, B. Chinna Babu, B. Siddhardha, U. S. Murthy, Y. Venkateswarlu, *Eur. J. Med. Chem.* **2010**, 45, 4657–4663.
- [3] a) N. Kudo, N. Matsumori, H. Taoka, D. Fujiwara, E. P. Schreiner, B. Wolff, M. Yoshida, S. Horinouchi, *Proc. Natl. Acad. Sci. USA* **1999**, 96, 9112–9117; b) T. Meissner, E. Krause, U. Vinkemeier, *FEBS Lett.* **2004**, 576, 27–30; c) M. Kalesse, M. Christmann, U. Bhatt, M. Quitschalle, E. Claus, A. Saeed, A. Burzlaff, C. Kasper, L. O. Haustedt, E. Hofer, T. Scheper, W. Beil, *ChemBioChem* **2001**, 2, 709–714.
- [4] a) M. J. Evans, B. F. Cravatt, *Chem. Rev.* **2006**, 106, 3279–3301; b) M. Fonovic, M. Bogoy, *Curr. Pharm. Des.* **2007**, 13, 253–261.
- [5] F. Allais, M. Aouhansou, A. Majira, P. H. Ducrot, *Synthesis* **2010**, 2787–2793.
- [6] D. K. Mohapatra, P. P. Das, D. S. Reddy, J. S. Yadav, *Tetrahedron Lett.* **2009**, 50, 5941–5944.
- [7] D. K. Reddy, V. Shekhar, T. S. Reddy, S. P. Reddy, Y. Venkateswarlu, *Tetrahedron: Asymmetry* **2009**, 20, 2315–2319.
- [8] D. Bose, E. Fernandez, J. Pietruszka, *J. Org. Chem.* **2011**, 76, 3463–3469.
- [9] a) J. S. Cannon, S. F. Kirsch, L. E. Overman, H. F. Sneddon, *J. Am. Chem. Soc.* **2010**, 132, 15192–15203; b) J. S. Cannon, S. F. Kirsch, L. E. Overman, *J. Am. Chem. Soc.* **2010**, 132, 15185–15191.
- [10] S. F. Kirsch, L. E. Overman, N. S. White, *Org. Lett.* **2007**, 9, 911–913.
- [11] K. M. Maloney, J. Y. Chung, *J. Org. Chem.* **2009**, 74, 7574–7576.

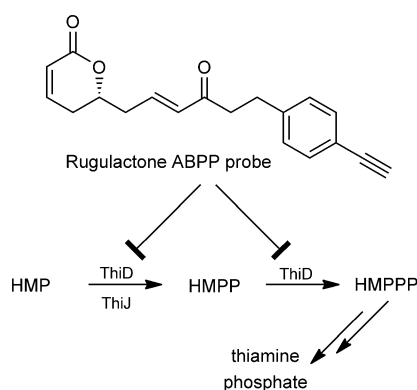
- [12] R. W. Ellis, *J. Antimicrob. Chemother.* **2003**, *51*, 739–740.
- [13] a) M. Meldal, C. W. Tornøe, *Chem. Rev.* **2008**, *108*, 2952–3015; b) V. V. Rostovtsev, L. G. Green, V. V. Fokin, K. B. Sharpless, *Angew. Chem.* **2002**, *114*, 2708–2711; *Angew. Chem. Int. Ed.* **2002**, *41*, 2596–2599; c) A. E. Speers, G. C. Adam, B. F. Cravatt, *J. Am. Chem. Soc.* **2003**, *125*, 4686–4687.
- [14] a) T. Böttcher, S. A. Sieber, *J. Am. Chem. Soc.* **2010**, *132*, 6964–6972; b) M. H. Kunzmann, I. Staub, T. Böttcher, S. A. Sieber, *Biochemistry* **2011**, *50*, 910–916.
- [15] S. J. Sasindran, S. Saikolappan, S. Dhandayuthapani, *Future Microbiol.* **2007**, *2*, 619–630.
- [16] T. M. Wizemann, J. Moskovitz, B. J. Pearce, D. Cundell, C. G. Arvidson, M. So, H. Weissbach, N. Brot, H. R. Masure, *Proc. Natl. Acad. Sci. USA* **1996**, *93*, 7985–7990.
- [17] a) J. M. Mei, F. Nourbakhsh, C. W. Ford, D. W. Holden, *Mol. Microbiol.* **1997**, *26*, 399–407; b) S. Dhandayuthapani, M. W. Blaylock, C. M. Bebear, W. G. Rasmussen, J. B. Baseman, *J. Bacteriol.* **2001**, *183*, 5645–5650.
- [18] T. T. Luong, P. M. Dunman, E. Murphy, S. J. Projan, C. Y. Lee, *J. Bacteriol.* **2006**, *188*, 1899–1910.
- [19] a) S. Ingavale, W. van Wamel, T. T. Luong, C. Y. Lee, A. L. Cheung, *Infect. Immun.* **2005**, *73*, 1423–1431; b) P. R. Chen, T. Bae, W. A. Williams, E. M. Duguid, P. A. Rice, O. Schneewind, C. He, *Nat. Chem. Biol.* **2006**, *2*, 591–595.
- [20] F. Sun, L. Zhou, B. C. Zhao, X. Deng, H. Cho, C. Yi, X. Jian, C. X. Song, C. H. Luan, T. Bae, Z. Li, C. He, *Chem. Biol.* **2011**, *18*, 1032–1041.
- [21] W. Du, J. R. Brown, D. R. Sylvester, J. Huang, A. F. Chalker, C. Y. So, D. J. Holmes, D. J. Payne, N. G. Wallis, *J. Bacteriol.* **2000**, *182*, 4146–4152.
- [22] K. L. Blake, A. J. O'Neill, D. Mengin-Lecreulx, P. J. Henderson, J. M. Bostock, C. J. Dunsmore, K. J. Simmons, C. W. Fishwick, J. A. Leeds, I. Chopra, *Mol. Microbiol.* **2009**, *72*, 335–343.
- [23] T. P. Begley, D. M. Downs, S. E. Ealick, F. W. McLafferty, A. P. Van Loon, S. Taylor, N. Campobasso, H. J. Chiu, C. Kinsland, J. J. Reddick, J. Xi, *Arch. Microbiol.* **1999**, *171*, 293–300.
- [24] a) Q. Du, H. Wang, J. Xie, *Int. J. Biol. Sci.* **2011**, *7*, 41–52; b) G. Khare, R. Kar, A. K. Tyagi, *PLoS One* **2011**, *6*, e22441.
- [25] D. A. Rodionov, A. G. Vitreschak, A. A. Mironov, M. S. Gelfand, *J. Biol. Chem.* **2002**, *277*, 48949–48959.
- [26] K. Schauer, J. Stolz, S. Scherer, T. M. Fuchs, *J. Bacteriol.* **2009**, *191*, 2218–2227.
- [27] M. G. Vander Heiden, H. R. Christofk, E. Schuman, A. O. Subtelny, H. Sharfi, E. E. Harlow, J. Xian, L. C. Cantley, *Biochem. Pharmacol.* **2010**, *79*, 1118–1124.
- [28] a) C. Avonto, O. Tagliatela-Scafati, F. Pollastro, A. Minassi, V. Di Marzo, L. De Petrocellis, G. Appendino, *Angew. Chem.* **2011**, *123*, 487–491; *Angew. Chem. Int. Ed.* **2011**, *50*, 467–471; b) S. Amslinger, *ChemMedChem* **2010**, *5*, 351–356.
- [29] G. Cheng, E. M. Bennett, T. P. Begley, S. E. Ealick, *Structure* **2002**, *10*, 225–235.
- [30] S. A. Sieber, S. Niessen, H. S. Hoover, B. F. Cravatt, *Nat. Chem. Biol.* **2006**, *2*, 274–281.

Received: April 20, 2012

Published online on ■■■■■, 0000

FULL PAPERS

Target acquisition: Rugulactone, a plant natural product isolated in 2009, has been reported to display interesting biological properties, but its protein targets in biological systems have not been examined. We have applied activity-based protein profiling to examine the targets of rugulactone in bacteria and have found that inhibition of thiamine biosynthesis contributes to its antibacterial activity.



*M. B. Nodwell, H. Menz, S. F. Kirsch,
S. A. Sieber**

■■ – ■■

Rugulactone and its Analogues Exert Antibacterial Effects through Multiple Mechanisms Including Inhibition of Thiamine Biosynthesis

